This article was downloaded by:
On: *28 January 2011*
Access details: *Access Details: Free Access*
Publisher *Taylor & Francis*
Informa Ltd Registered in England and Wales Registered Number: 1072954 Registered office: Mortimer House, 37-41 Mortimer Street, London W1T 3JH, UK

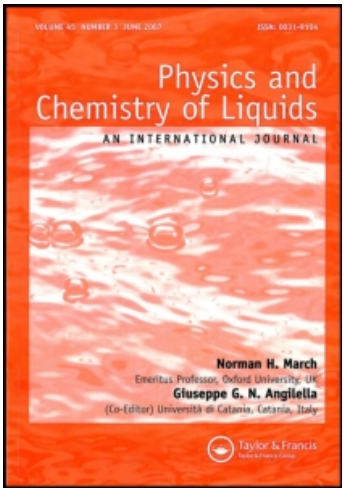

Physics and Chemistry of Liquids
Publication details, including instructions for authors and subscription information:
http://www.informaworld.com/smpp/title~content=t713646857

Structure of Molten Copper-Antimony Alloys by Combination of Neutron and X-ray Diffraction

Walter Knoll[a]; Siegfried Steeb[a]
[a] Max-Planck-Institut für Metallforschung Institut für Sondermetalle, Stuttgart, West Germany

To cite this Article Knoll, Walter and Steeb, Siegfried(1973) 'Structure of Molten Copper-Antimony Alloys by Combination of Neutron and X-ray Diffraction', Physics and Chemistry of Liquids, 4: 1, 39 — 60
To link to this Article: DOI: 10.1080/00319107308083822
URL: http://dx.doi.org/10.1080/00319107308083822

PLEASE SCROLL DOWN FOR ARTICLE

Full terms and conditions of use: http://www.informaworld.com/terms-and-conditions-of-access.pdf

This article may be used for research, teaching and private study purposes. Any substantial or systematic reproduction, re-distribution, re-selling, loan or sub-licensing, systematic supply or distribution in any form to anyone is expressly forbidden.

The publisher does not give any warranty express or implied or make any representation that the contents will be complete or accurate or up to date. The accuracy of any instructions, formulae and drug doses should be independently verified with primary sources. The publisher shall not be liable for any loss, actions, claims, proceedings, demand or costs or damages whatsoever or howsoever caused arising directly or indirectly in connection with or arising out of the use of this material.

Physics and Chemistry of Liquids. 1973. Vol.4, pp. 39–60
Copyright © 1973 Gordon and Breach Science Publishers
Printed in Great Britain

Structure of Molten Copper–Antimony Alloys by Combination of Neutron and X-ray Diffraction

WALTER KNOLL and SIEGFRIED STEEB

Max-Planck-Institut für Metallforschung
Institut für Sondermetalle
Stuttgart, West Germany

Abstract—Diffraction experiments with 21 alloys from the system Cu–Sb were done by means of neutrons (1.19 Å) in transmission and by X-rays in reflection (Mo K_α, θ–θ goniometer). Corrections for neutron diffraction data are given and the RDF were calculated. Discussion of the nearest neighbours' distance r_I and the coordination number z versus the concentration was done. With variation of the concentration the melts show compound formation, segregation tendency or statistical distribution of the atoms of both components. The quantitative subdivision of the melts with 15 up to 61 a/o Sb into two structural components shows that the melts with 44 a/o Sb contain up to 37 Mol% of Cu_2Sb agglomerates.

The combination of X-ray and neutron-diffraction data yielded that the Sb atoms as well as the Cu atoms in the molten alloys with 52 up to 90 a/o Sb show the same distances as with the melts of the pure metals. Viscosity measurements done by other workers can be explained by the structural results.

Downloaded At: 09:02 28 January 2011

1. Introduction

Recent progress in experimental equipment allows to investigate molten alloys of complex systems with high melting points. Normally, X-ray or neutron diffraction is done. Henninger, Buschert, and Heaton[1] for the first time used both methods. This was also done in the present work and comparison of the results obtained by both methods should give more information concerning the atomic arrangement in the molten state.

The system Cu–Sb was chosen because Cu shows a larger scattering amplitude for neutrons than Sb, whereas Sb shows a larger scattering amplitude for X-rays than Cu. Thus it was to be expected that the neutrons reveal more information concerning the Cu atoms, whereas the X-rays give more details concerning the Sb atoms.

2. Theoretical Outline

The coherent scattered intensity is described according to Ref. 2 for the X-ray and neutron diffraction, the scattering power of a single atom being given by the angle dependent atomic scattering factor in the first case and by the angle independent scattering amplitude in the latter case. According to Ref. 2 also the interference and the shortened functions were calculated from the intensity curves.

Furthermore by Fourier transformation the RDF and paircorrelation functions were obtained.

Corrections

Concerning the corrections for the neutron-intensity curves the following should be stated:

Besides the wanted coherent scattered intensity I_{coh} of the specimen the measured intensity curves I_{exp} contain further fractions, which are to be eliminated by correction procedures. This will be done in the following sequence:

(a) Background scattering from the surroundings,
(b) Background scattering from the cuvette and the furnace including absorption in cuvette and furnace,
(c) Absorption in the specimen,
(d) Angle dependent sensitivity of the goniometer,
(e) Multiple scattering from the specimen,
(f) Incoherent scattering from the specimen.

The total coherent, incoherent, and multiple scattered intensity $I_{corr}(s)$ from the specimen can be described as follows:

$$I_{corr}(s) = A \cdot V_c \cdot \left[I_{exp} - \left(I_b + \frac{I_{Cd}}{V_c} + \frac{I_{cuv} - I_{Cd}}{A \cdot V_c} \right) \right] \tag{1}$$

with V_c = Vanadium correction for the sensitivity of the goniometer,
A = absorption factor,
I_{exp} = measured intensity,
I_b = background intensity,
I_{Cd} = intensity from a cuvette filled with Cd,
I_{cuv} = intensity from an empty cuvette.

Downloaded At: 09:02 28 January 2011

(a) Before and after each measurement the background scattering was measured with closed neutron source for the angles $2\theta = 0°$, $60°$ and $120°$. These values showed only small deviations and therefore the constant amount I_b could be subtracted from the total measured intensity. ($I_b \approx 90$ to 270 pulses/measurement.)

(b) To get I_{cuv} and I_{Cd}, the absorption of the cuvette must be observed and the measurement of the following intensities was necessary:

(α) Empty cuvette (SiO_2) $\quad I_{cuv}$

(β) Cuvette filled with Cd $\quad I_{Cd}$

The absorption cross section of Cd for thermal neutrons amounts to $\sigma = 2650$ barn and therefore can be regarded as totally absorbing medium. The intensity I_{Cd} measured with the arrangement (β) therefore arises from those parts of the cuvette and the furnace where only those neutrons are scattered which neither before nor after the scattering process transmit the specimen and therefore also are not absorbed. This intensity I_{Cd} is subtracted from the intensity I_{cuv}. The difference ($I_{cuv} - I_{Cd}$) must be corrected for absorption in the specimen, since this fraction of intensity is given by those neutrons which transmit the specimen during the effective diffraction experiment. For correction this intensity is divided by the absorption factor A (Eq. (1)) and furthermore by the goniometer correction V_c. The absorption within the radiation window and the heating tube of the furnace can be neglected.

(c) The absorption correction A for cylindrical specimens which are fully bathed by the beam was given by Bradley.[3] According to Ref. 3 A is a complex function of the product $R \cdot \mu$ and of the amount of scattering vector s (with R = radius of specimen and μ = attenuation coefficient). These parameters are tabulated[4] and the expression

$$A = f(\mu \cdot R, s) \tag{2}$$

holds.

To determine A, the attenuation coefficient μ is needed. This was done by experiment and by calculation:

$$\mu = N_A \cdot \sum_{i=1}^{2} \frac{c_i \sigma_{T_i} D_i}{A_i} \tag{3}$$

Downloaded At: 09:02 28 January 2011

with N_A = Avogadro's number,
D_i = partial density of component i,
c_i = atomic concentration of component i,
σ_{T_i} = total cross section for thermal neutrons,
A_i = atomic weight of component i.

The partial densities of the components were determined according to Ref. 5 using the experimental molar volumina given in Ref. 6. For copper, the value of the absorption coefficient A varies in the region from $s = 0$ up to $s = 9.1$ Å^{-1} at 17%; for antimony, however, only at 1.2%. The alteration for the alloys lies between these two borders.

(d) To determine an eventual angle dependent sensitivity of the goniometer, a Vanadium-cylinder with the same dimensions as the liquid specimen was investigated within the apparatus. V shows a negligible coherent scattering cross section. Therefore the measured intensity is due to incoherent scattering including a multiple scattered component, which should be angle independent. The actually measured angle-dependency therefore means an angle dependent sensitivity of the goniometer.

To check the described corrections, the intensity of a Vanadium specimen in a silica tube was measured and these results corrected by using Eq. (1). The corrected intensity showed complete agreement with the intensity from a Vanadium specimen solely, which was only corrected for A and V_c.

Therefore the correction proposed by Paalman and Pings[7] for specimens in silica tubes[8] was not applied. In the following the corrections needed for the transformation of I_{corr} into I_{coh} are described.

(e) By multiple scattering I_M the angle distribution of the scattered neutrons is influenced in such a way that the maxima are obtained too flat. It is of special interest during the examination of single crystal and powder specimens, whereas during the examination of melts with their relative weak maxima its influence is small. According to Vineyard[9] it can be neglected if the transmission amounts to 90%. For the radii of the investigated specimens of about 1 cm the transmission lies between 60% (for Cu) and 78% (for Sb). Concerning the relative high absorption in the investigated specimens, multiple scattering can be considered as isotrope. The scattering

Downloaded At: 09:02 28 January 2011

cross section σ_M for multiple scattering for the different concentrations was calculated according to Ref. 10.

(f) The incoherent scattering I_{inc} from the specimen can be considered as isotrope background scattering. It consists according to Ref. 11 of an elastic and an inelastic part and is described in Ref. 11 for each element by the scattering cross section σ_{inc}.

NORMALIZATION PROCEDURE

The coherent scattered intensity is given by

$$I_{\text{coh}}(s) = I_{\text{corr}}(s) - (I_{\text{inc}} + I_M) \tag{4}$$

The intensities in parentheses are angle-independent. The coherent scattering intensity must approach zero for small scattering angles[12] if the melt contains no clusters. Furthermore there exists an amount of zero angle scattering to be neglected here, which arises from the isothermal compressibility of the melt. With binary melts furthermore the so called Laue monotonic scattering I_{LMS} arises:

$$I_{\text{LMS}} = \langle b^2 \rangle - \langle b \rangle^2 \tag{5}$$

The total zero angle intensity for melts without clusters therefore becomes:

$$I_{\text{corr}}(0) = I_{\text{inc}} + I_M + I_{\text{LMS}} \tag{6}$$

For the correction according to Eq. (4) from these intensities only the two terms are needed:

$$I(0) = I_{\text{inc}} + I_M \tag{7}$$

There is a difficulty in determining $I(0)$ since the measurement only can start at $s = 0.5$ Å^{-1}. Therefore the intensity curves I_{corr} must be extrapolated to $s = 0$. This is only possible in an arbitrary manner, since the measured values between $s = 0.5$ Å^{-1} and 1.0 Å^{-1} are not too precise.

Therefore the exactly known or calculated scattering cross sections were used to determine $I(0)$ in the following way:

$s \to \infty$ yields

$$I_{\text{corr}}(\infty) = I_{\text{coh}}(\infty) + I(0) = \text{const.} \tag{8}$$

Forming the quotient k from $I_{\text{coh}}(\infty)$ and $I(0)$, the intensities can be replaced by the scattering cross sections. For a binary system

Downloaded At: 09:02 28 January 2011

the following relation stands:

$$k = \frac{I_{\text{coh}}(\infty)}{I(0)} = \sum_{i=1}^{2} \frac{c_i \sigma_{\text{coh}}^i}{\sigma_{\text{inc}}^i + \sigma_M{}^i} \tag{9}$$

with c_i = atomic concentration,

σ_{coh}^i, σ_{inc}^i = coherent and incoherent, respectively, scattering cross sections of atoms of the component i for thermal neutrons[11]

$\sigma_M{}^i$ = calculated cross section for multiple scattering.[10]

From Eq. (8) and (9) follows:

$$I(0) = \frac{I_{\text{corr}}(\infty)}{k+1} \tag{10}$$

With this equation the intensity $I(0)$ is reduced by means of the ratio k to the intensity $I_{\text{corr}}(\infty)$ at infinite scattering angle, which was determined in the present work using an altered Norman[13] and Krogh-Moe[14] method.

The intensity curves are extrapolated to $I(0)$ by a parabola which starts from $I(0)$ along a horizontal tangent up to the first exactly measured values of intensity:

$$I_{\text{corr}}(s) = a \cdot s^2 + I(0) \tag{11}$$

For the calculation of the intensity at large scattering angles the treatment according to Refs. 13 and 14 was altered using the fact that also the RDF must approach zero for $r \to 0$. This yields

$$\int_0^\infty s \cdot F(s)\, \mathrm{d}s = -2\pi^2 \rho_0 \tag{12}$$

with ρ_0 = mean atomic density,

F = shortened interference function.

Since the experiments only can be performed up to $s_{\max}$, this value is used as an upper integration limit. Finally one gets:

$$I_{\text{corr}}(\infty) = \frac{\int_0^{s_{\max}} s^2 I_{\text{corr}}(s)\, \mathrm{d}s - 2\pi^2 \rho_0 I_{\text{LMS}}}{(1/3)s_{\max}^3 - 2\pi^2 \rho_0 (k/k+1)} \tag{13}$$

Thus the functions $I(0)$, $F(s)$ etc. can be calculated.

3. Experiments

Twelve different specimens were prepared for the neutron diffraction experiments. As initial substances, copper (99.9%, granulated)

Downloaded At: 09:02 28 January 2011

and antimony (99.8%, As ~0.05%, Pb ~0.1%, and Fe ~0.01%) were used. The specimens were casted in a vacuum induction furnace and sealed into evacuated silica tubes so that the specimen diameters approached optimum thickness.

For the X-ray experiments nine specimens were prepared with special regard to the antimony rich part of the phase diagram (Fig. 1). The crucibles consisted of graphite.

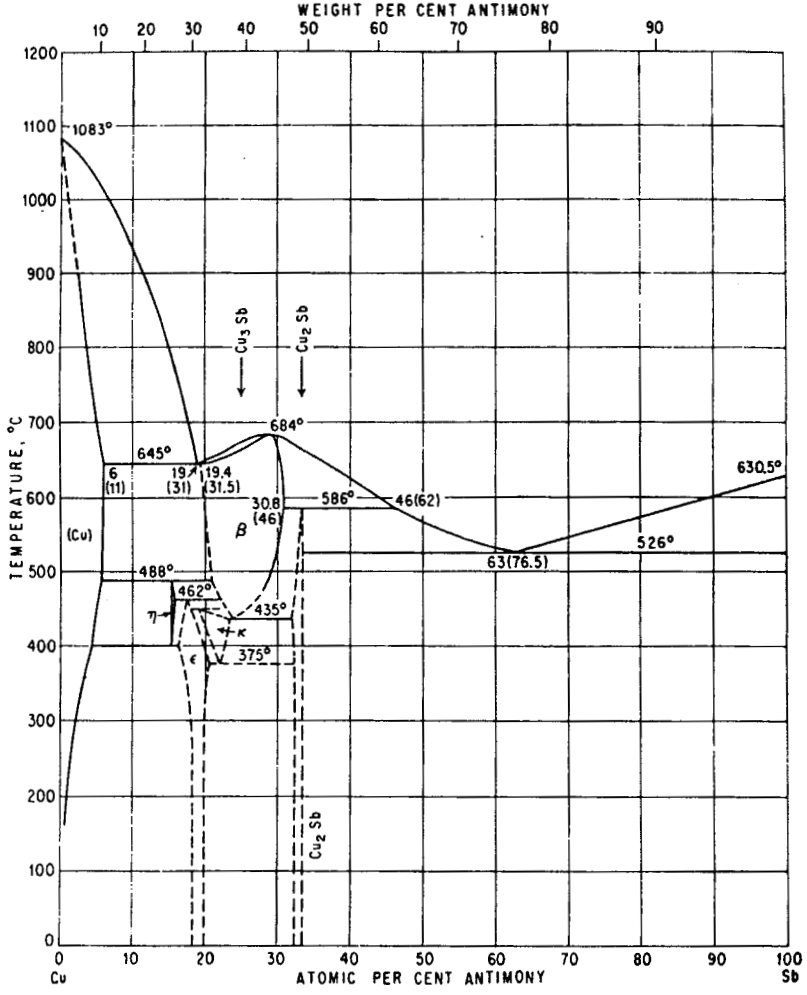

Figure 1. Phase diagram of the system Cu–Sb.[15]

Downloaded At: 09:02 28 January 2011

All specimens showed during the whole measurement a bright surface so that the results are not influenced by oxide layers.

For the neutron diffraction experiments a device was used which is similar to the diffractometer shown in Fig. 5(ii) of Ref. 11. Instead of one counter, however, in our case four BF_3-counters with a fixed distance of $2\theta = 15°$ were used. Furthermore the device works fully automatically by tape control. It is installed at the research reactor FR 2 at Karlsruhe. The goniometer bears a heating unit which was built according to Ref. 16 and the whole set works in transmission. The silica-cuvettes were placed within a cylinder of Vanadium foil, which was heated by direct current.

Maximum specimen temperature amounted up to 1200 °C with a variation of ± 5 °C/48 h. The furnace runs at 10^{-5} Torr. The neutrons were monochromatized ($\lambda = 1.19$ Å ± 1.5%) by reflection at the (111)-planes of a lead-single crystal used in transmission.

The X-ray diffraction experiments were done with a θ–θ goniometer in which the horizontal surface of the melts can be investigated in Bragg–Brentano focusing condition. The construction and function of this instrument is described in Ref. 17.

After melting and heating the specimen to a temperature 50 °C above the temperature of investigation, this temperature was approached from this higher value. All specimens were investigated 10° above liquidus, some of them 200° above liquidus. The scattered neutron intensity was registered in the region $5° \leq 2\theta \leq 120°$ corresponding to $0.5 \leq s \leq 9.1$ Å^{-1} in steps of $\Delta 2\theta = 0.2°$ using pulse preset, the statistical error being less than 1.6%.

Concerning the X-ray experiments see Ref. 6. These measurements were done using Argon-atmosphere in the region $1.4 \leq s \leq 13.5$ Å^{-1} in steps of $\Delta s = 0.04$ Å^{-1} with a statistical error of maximum 1.6%.

4. Results and Discussion

Figures 2 and 3 show the corrected and normalized neutron intensity curves for twelve molten alloys from the system Cu–Sb. The solid lines were measured at 10 °C and the dashed lines at 200 °C above liquidus. Figure 4 shows the corrected and normalized X-ray intensity curves for nine different alloys.

Downloaded At: 09:02 28 January 2011

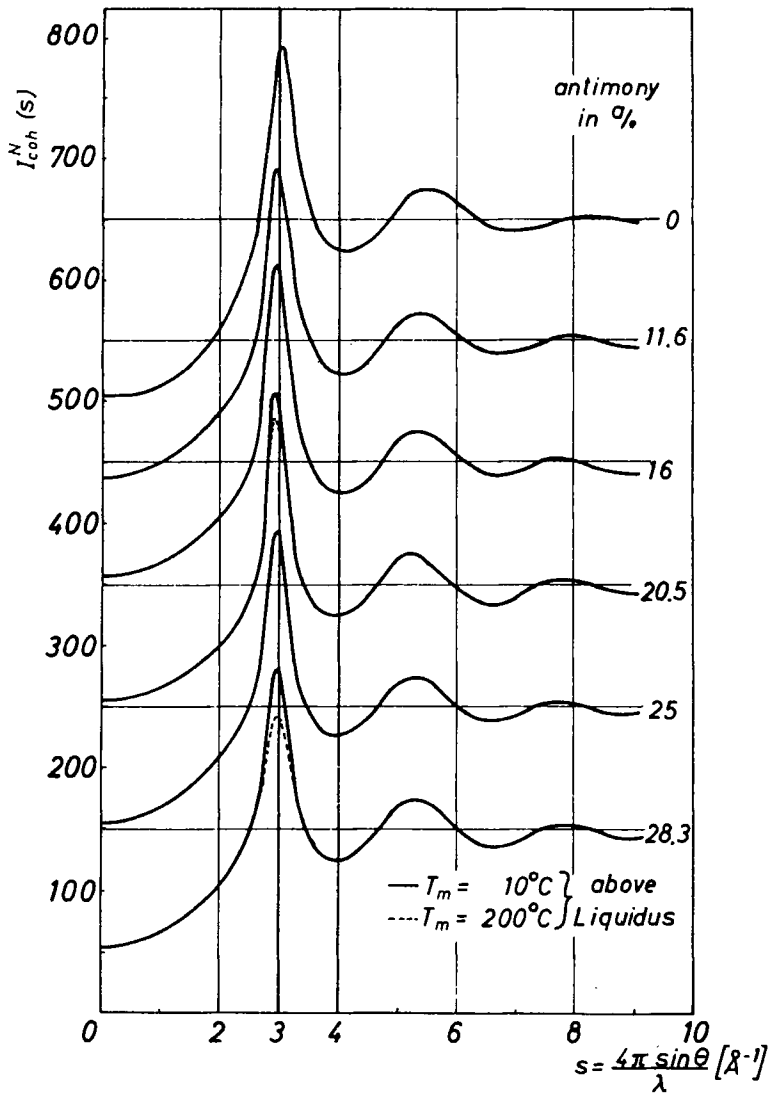

Figure 2. System Cu–Sb: Intensity curves in the region 0 up to 28.3 a/o Sb. (Neutron diffraction.)

Downloaded At: 09:02 28 January 2011

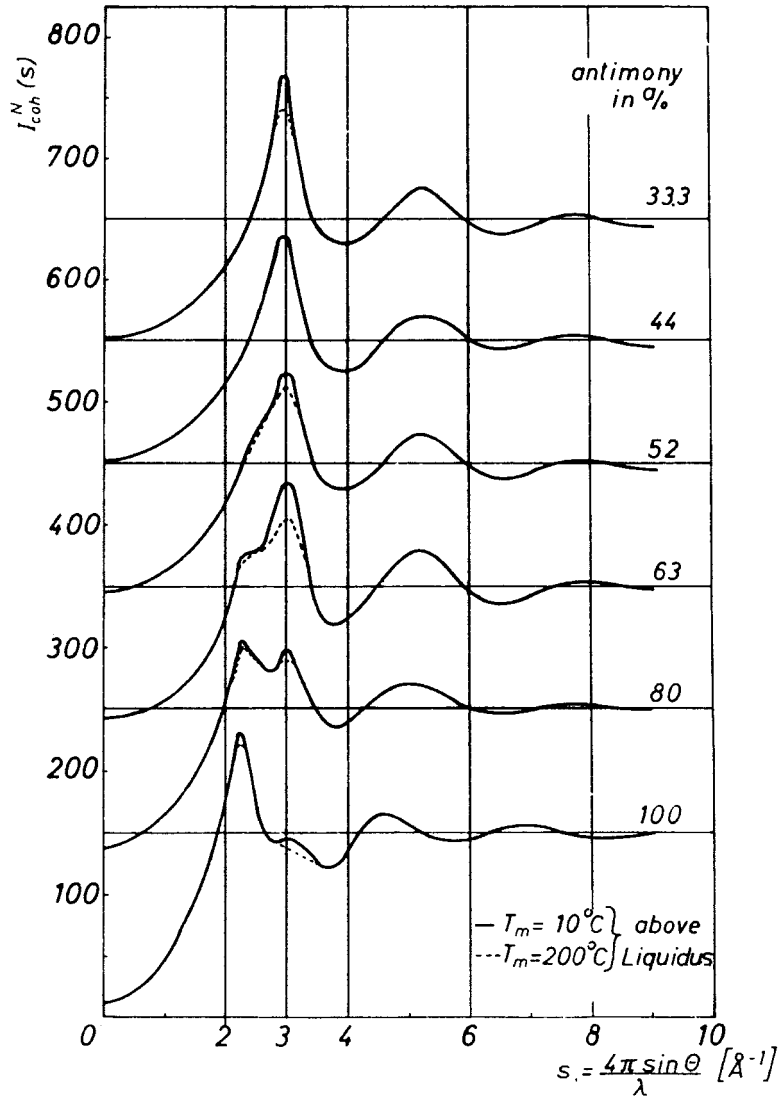

Figure 3. System Cu–Sb: Intensity curves in the region 33.3 up to 100 a/o Sb. (Neutron diffraction.)

Downloaded At: 09:02 28 January 2011

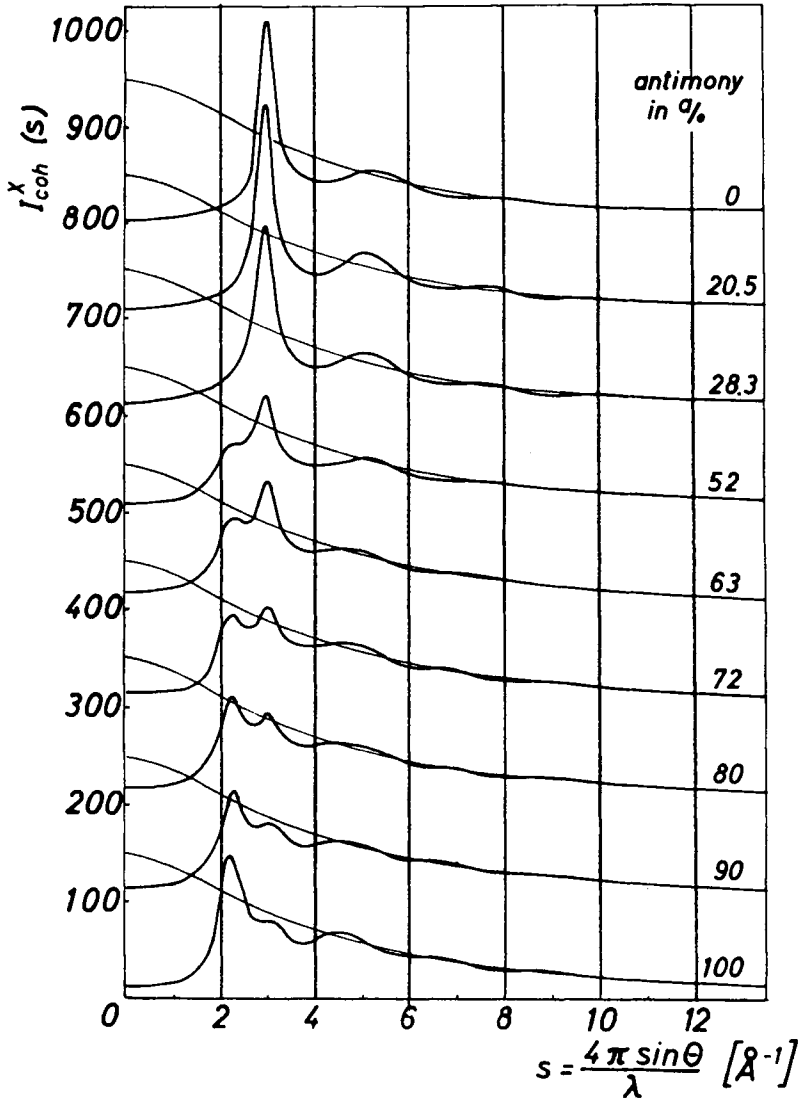

Figure 4. System Cu–Sb: Intensity curves. (X-ray diffraction.)

Downloaded At: 09:02 28 January 2011

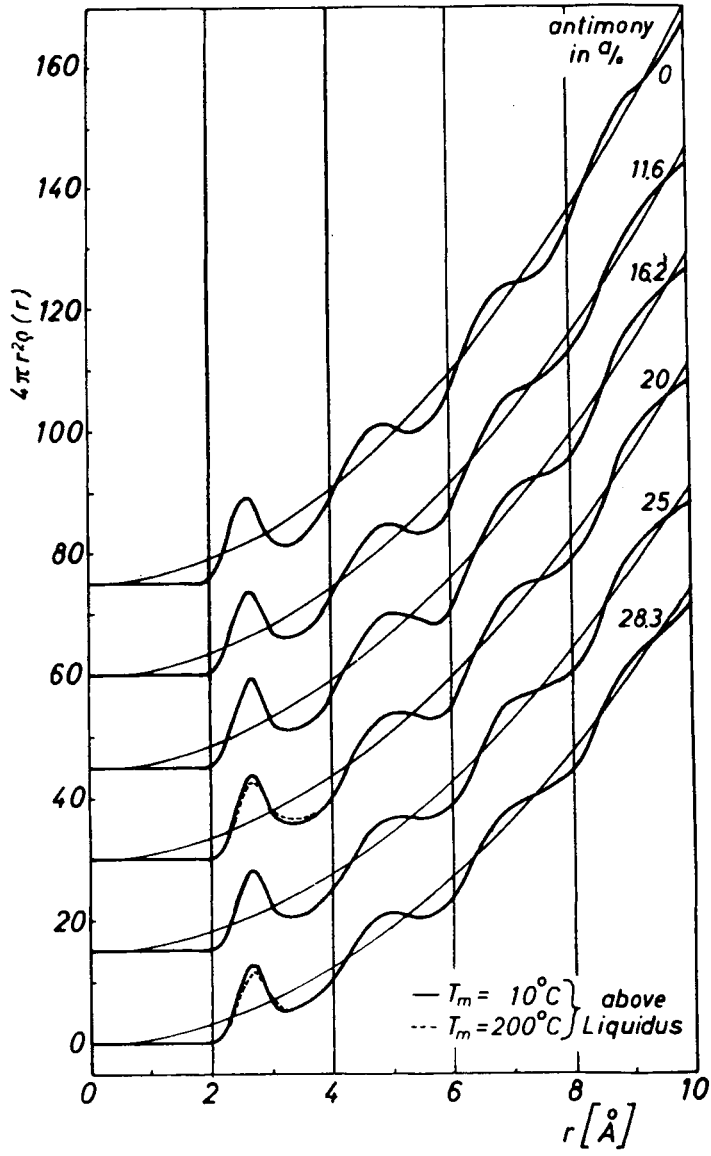

Figure 5. System Cu–Sb: RDF in the region 0 up to 28.3 a/o Sb. (Neutron diffraction.)

Downloaded At: 09:02 28 January 2011

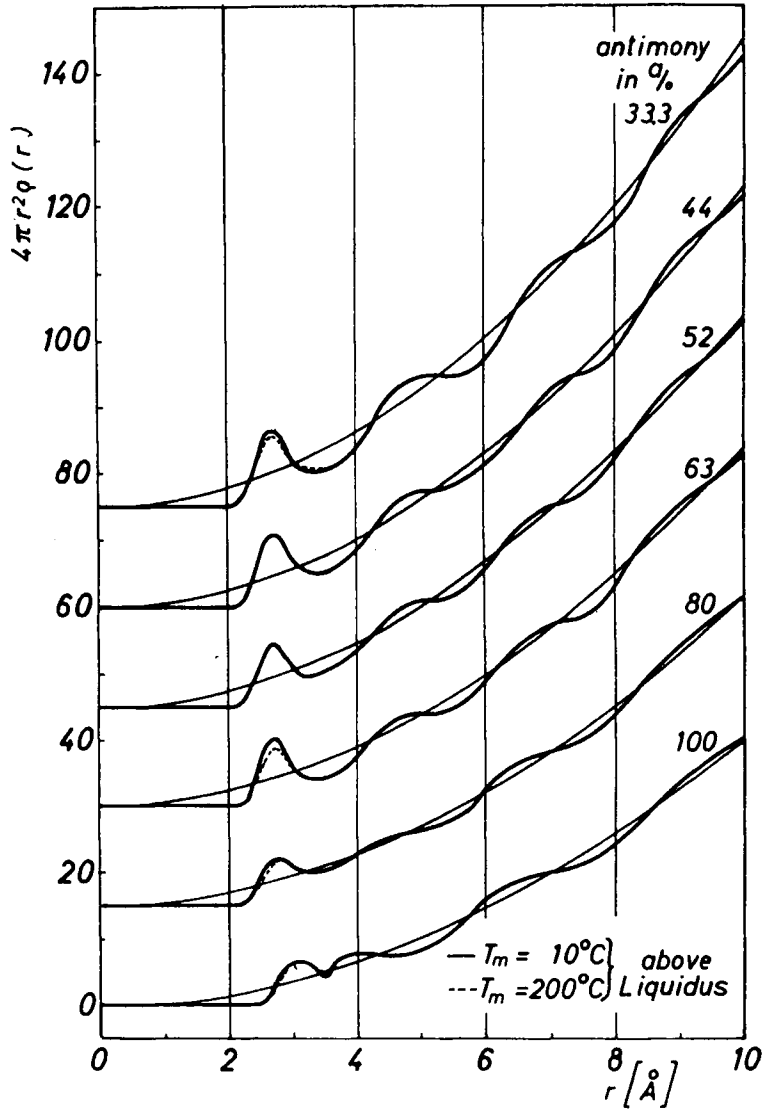

Figure 6. System Cu–Sb: RDF in the region 33.3 up to 100 a/o Sb. (Neutron diffraction.)

Downloaded At: 09:02 28 January 2011

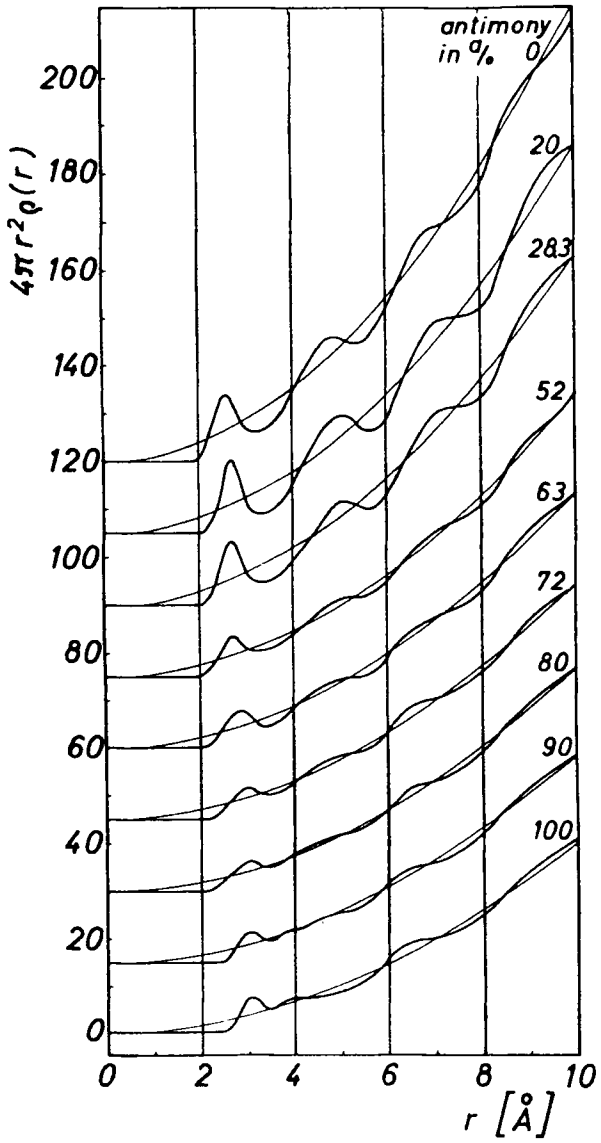

Figure 7. System Cu–Sb: RDF (X-ray diffraction).

Downloaded At: 09:02 28 January 2011

The RDF are shown for neutrons in Figs. 5 and 6 and for X-rays in Fig. 7.

The intensity curves of the pure components are very different (compare Figs. 2, 3 and 4). Furthermore a splitting of the first intensity maximum with the alloys in the range of 52 up to 90 a/o Sb occurs. Both effects are observed for neutrons as well as for X-rays. The intensity curve of pure antimony has its first maximum at $s = 2.2$ Å^{-1}. The position of the first maximum at 2.16 up to 2.18 Å^{-1} given in Refs. 18 to 21 shows only a small deviation from the present value. An additional maximum is found at $s = 3.1$ Å^{-1}. This maximum also was observed in Refs. 18 to 21 and is ascribed in Ref. 19 to the strong maximum at 3.3 Å^{-1} observed with amorphous antimony. The structure of the amorphous phase was, however, not discussed in terms of the molten phase in Ref. 19.

In the present work the interference function of antimony was Fourier-transformed once with and once without the additional maximum. The obtained RDF, however, showed no alteration; especially at r-values smaller r_I no anomalies could be observed. Therefore the existence of an additional intensity maximum cannot be connected with the appearance of a small atomic distance.

The intensity curve of copper shows the run expected for a molten element with $s_I = 3.02$ Å^{-1} which is in agreement with the value $s_I = 2.96$ Å^{-1} reported in Ref. 22.

With the alloys, those of high antimony concentration are of special interest. Between 52 and 90 a/o Sb a splitting of the first intensity maximum occurs. At 90 a/o Sb only an enlargement of the additional maximum of the intensity curve of pure antimony seems to occur. However, the high angle part of the split maximum is shifted to $s = 2.98$ Å^{-1}. Furthermore, its height is dependent on the copper concentration. The same stands for the low angle part of the split maximum.

It is of interest to compare the intensity curves obtained with neutron or X-rays, respectively, at alloys with 52 a/o Sb. The X-ray curve shows a maximum at $s = 2.2$ Å^{-1}; that means at the value of the first maximum of Sb, whereas this maximum is only indicated in the neutron curve. This can be explained by the different scattering power of Cu- or Sb-atoms for X-rays and neutrons. (X-rays: $I_{Sb}/I_{Cu} \approx 1.75$; neutrons: $I_{Sb}/I_{Cu} \approx 0.47$).

Downloaded At: 09:02 28 January 2011

As a whole the intensity curves show that the melts between 52 and 90 a/o Sb contain two structural components, one of which shows maximum intensity at the same s-value as pure antimony, the second of which at the s-value of pure copper or the intermetallic compound Cu_2Sb. The phase diagram (Fig. 1) shows an eutecticum at 63 a/o Sb. Therefore it can be assumed that the melt is segregated into regions rich in copper or antimony, respectively.

To estimate the degree of segregation, intensity curves for total segregation were calculated by weighted superposition of the intensity curves of the pure components. These calculated curves were in good agreement with the measured curves. The calculated ones however showed a more pronounced dip between the first two maxima than the measured ones. Thus it is to be stated that apparently the melts are not completely segregated.

The RDF presented in Figs. 5, 6 and 7 show the usual run. Especially no splitting of the first maximum is obtained as to be expected from the intensity curves with Sb concentrations between 52 and 90 a/o. From these curves the distance r_I and number z of nearest neighbour atoms can be obtained.

Figure 8 shows in full line the run of the measured coordination

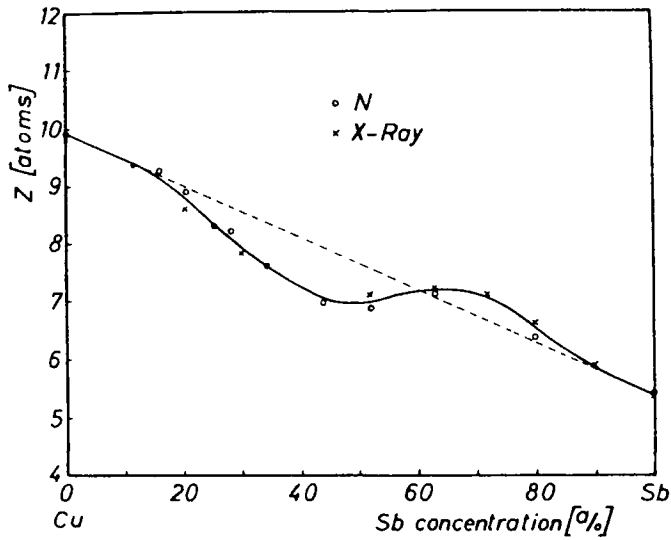

Figure 8. Number z of atoms in the first coordination sphere versus Sb concentration.

Downloaded At: 09:02 28 January 2011

number z versus alloy concentration. X-ray and neutron values are in good agreement. For the pure components Cu and Sb the coordination numbers 9.9 and 5.4, respectively, were obtained. The dashed line in Fig. 8 gives the value expected for the coordination number of alloys with statistical distribution of atoms. If the experimental value lies beneath this line, compound formation is indicated.[23] If the experimental value lies above the dashed line, there is segregation tendency in the melt.[23] Thus in accordance with the phase diagram (Fig. 1) the alloys from 15 up to 61 a/o Sb show compound formation. The alloys with less than 15 and more than 90 a/o Sb show statistical distribution of the atoms, whereas between 61 and 90 a/o Sb segregation tendency can be stated. Thus the segregation tendency already concluded from the intensity curves is proved also by aid of the coordination number z in the region from 61 up to 90 a/o Sb. It should be mentioned, that with the intensity curves the split of the first maximum already occurred at 52 a/o Sb. This difference can be explained by the simultaneous existence of compound regions and segregation regions within the melts with up to 61 a/o Sb.

In Ref. 24 a method was given for the quantitative subdivision of a melt showing compound formation into two structural components, one component consisting of atoms in statistical arrangement, the other component consisting of atoms arranged in a quite similar manner as in the solid compound of the same concentration as the whole melt. In the present case, this compound will be Cu_2Sb.† The result of the corresponding calculation is shown in Fig. 9.

The curves marked with a_{Cu} and a_{Sb} represent that part of copper or antimony atoms, respectively, which form the component with statistical distribution. For this calculation the segregation tendency of the melts with 61 up to 90 a/o Sb must be replaced by a statistical arrangement. The curve marked with a_{Cu_2Sb} represents that part of atoms which form within the melt molecules of the composition Cu_2Sb.

According to Fig. 9 the region, where the compound-like regions

† Equation (22) in Ref. 24 should read:

$$u = \frac{z_A - w(z_A - z_B) - z_{exp}}{z_A + \beta z_B - (1+\beta) z_{AB_\beta}}$$

Downloaded At: 09:02 28 January 2011

exist reaches from 15 up to 61 a/o Sb which is in good agreement with the phase diagram. Maximum of compound formation is found at 43 a/o Sb, where the agglomerates form 37% of the total melt.

Figure 10 shows the radius r_I versus the concentration. The X-rays as well as the neutrons exhibit for the pure components Cu

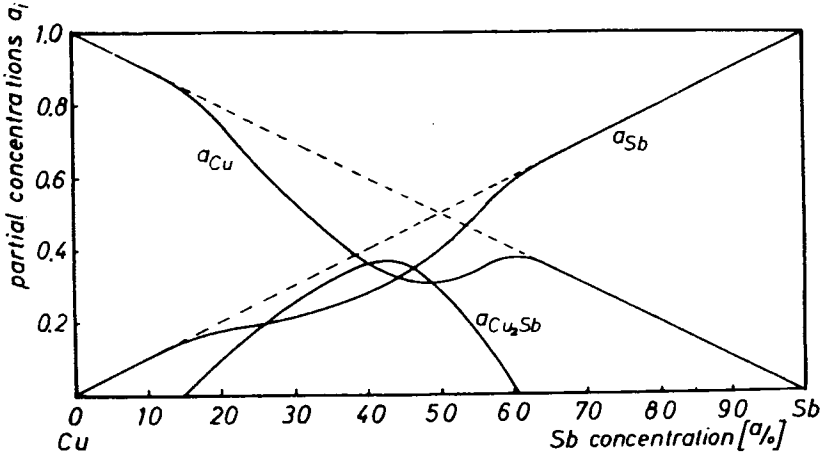

Figure 9. Quantitative subdivision of molten Cu–Sb alloys into two structural components.

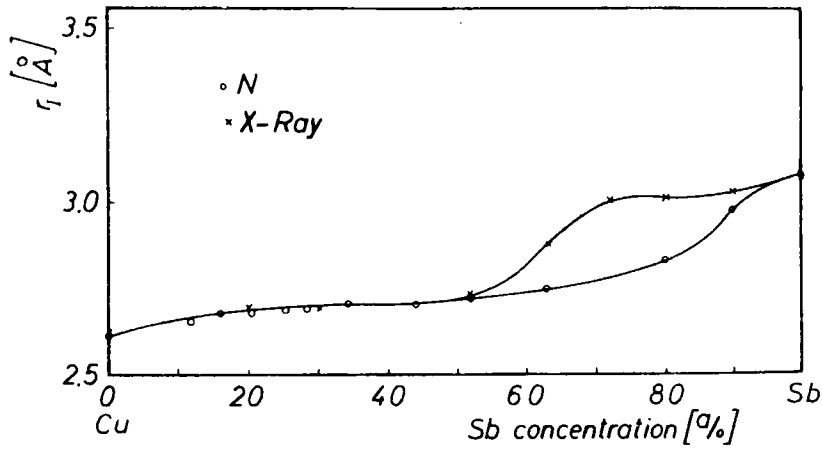

Figure 10. Experimental values r_I of the first coordination sphere.

Downloaded At: 09:02 28 January 2011

and Sb as well as for the alloys with up to 55 a/o Sb the same values of r_I. The r_I-values for Cu (2.61 Å) and for Sb (3.08 Å) are in good accordance with the values given in Refs. 22 and 19. Between 55 and 90 a/o Sb there is a great difference between the r_I values obtained from X-ray or neutron diffraction. The X-ray values are larger than the neutron values. An explanation for this discrepancy is given by the difference in the scattering strength of Cu and Sb for neutrons and X-rays. During the X-ray experiment, a Sb–Sb pair of atoms shows three times the scattering power of a Cu–Cu pair of atoms. Therefore the Sb–Sb distance in the RDF is maintained down to 70 a/o Sb. This tendency is supported by the strong segregation in this range of concentration. During the neutron diffraction experiment, on the other hand, the tendency prevails to maintain the Cu–Cu distance over the whole concentration range.

Downloaded At: 09:02 28 January 2011

Comparison of X-ray and Neutron Experiments

Comparison between the X-ray and the neutron-diffraction experiment is done according to Ref. 1, forming the quotient

$$R(r) = \frac{(c_1 f_1 + c_2 f_2)^2 \rho_{(r)}^{\text{X-ray}}}{(c_1 b_1 + c_2 b_2)^2 \rho_{(r)}^{N}(r)} \tag{14}$$

with ρ = measured atomic density.

This quotient shows different values according to the mutual arrangements of atoms in the melt. Figure 11 shows the expected value of R for the alloys 48 Cu 52 Sb and 20 Cu 80 Sb, if those contain Sb–Sb or Cu–Cu pairs only. The horizontal lines parallel to the abscissa correspond to statistical distribution of atoms. The run of $R(r)$ shows for the alloy with 80 a/o Sb a minimum at 2.63 Å, which indicates preferred formation of Cu–Cu pairs. The maxima at 3.09 Å and 3.80 Å show the preferred existence of Sb–Sb pairs.

These distances are in good accordance with the measured r_I values of the molten elements Cu (2.61 Å) and Sb (3.08 Å). According to Figs. 6 and 7 the maximum at 3.8 Å corresponds to the second maximum of the RDF of Sb. Similar considerations were done for the $R(r)$-curves with 63 and 52 a/o Sb. Finally it follows that for these concentrations the Cu and Sb atoms show the same distances as in the melts of the pure metals.

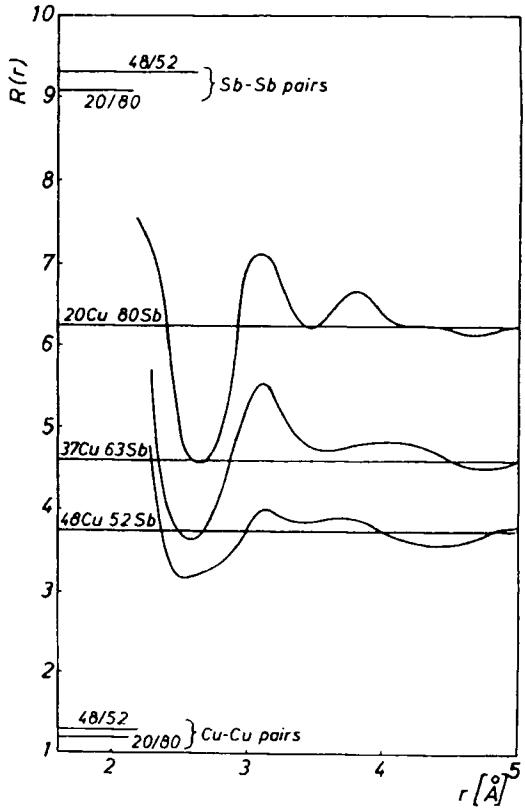

Figure 11. System Cu–Sb: Quotient $R(r)$ for three alloys (concentrations in a/o).

Structure and Viscosity

In Fig. 8 the tendency for compound formation in the Cu–Sb melts with 15 up to 61 a/o Sb was deduced. A confirmation of this fact is given by the run of the isotherms of viscosity at 1000 and 1188 °C, measured in Ref. 25 (compare Fig. 12a). These isotherms show at 35 a/o Sb a point of inflection and in the region of the intermetallic compound Cu_2Sb and the β-phase larger values than those expected for melts with statistical distribution of atoms (dashed line). For higher Sb concentrations, where segregation tendency is stated, these isotherms show the normal monotonous run. The isotherms of viscosity measured at 625 °C by Ref. 26 for alloys with 45 up to

Downloaded At: 09:02 28 January 2011

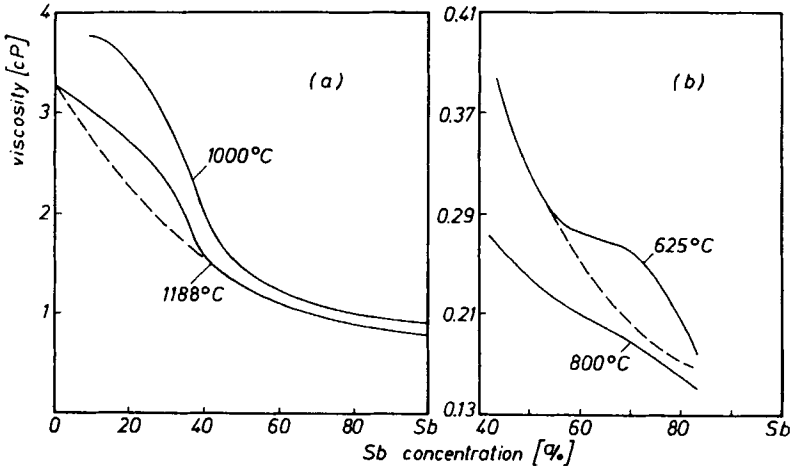

Figure 12. System Cu–Sb: Viscosity isotherms (a) according to Ref. 25, (b) according to Ref. 26.

Downloaded At: 09:02 28 January 2011

82 a/o Sb, however, (compare Fig. 12b), show at the eutectic composition a point of inflection and for the higher Sb concentrations larger values compared to the " normal " run. This fact is explained in Ref. 26 by the assumption of segregation also in the molten state, whereby the viscosity is enlarged by clusters. Thus the segregation tendency postulated in the present work for alloys with 61 up to 90 a/o Sb is confirmed by viscosity measurements. The run of the isotherm of viscosity for 800 °C in Fig. 12b shows no anomalies, i.e., at this temperature the atomic distribution within the melt tends to the statistical distribution.

Acknowledgements

Thanks are due to the " Deutsche Forschungsgemeinschaft ", the " Reaktor Bau- und Betriebs-Gesellschaft m.b.H., Karlsruhe ", and the " Rechenzentrum " of the University of Stuttgart.

REFERENCES

1. Henninger, E. H., Buschert, R. C. and Heaton, L., *Adv. Phys.* **16**, 177 (1967).

2. Kaplov, R., Strong, S. L. and Averbach, B. L. in " Local Atomic Arrangements studied by X-ray diffraction "; J. B. Cohen and J. E. Hilliard, Eds., Gordon and Breach, New York, 1966.
3. Bradley, A. J., *Proc. Phys. Soc. London* **47**, 879 (1935).
4. " International Tables of X-ray Crystallography ", Vol. II, p. 295.
5. Kortüm, G., " Einführung in die chemische Thermodynamik ", 4. Auflage, 1963, S. 75.
6. Bornemann, K. and Sauerwald, F., *Z. Metallkde.* **14**, 254 (1922).
7. Paalman, H. H. and Pings, C. J., *J. Appl. Phys.* **33**, 2635 (1962).
8. North, D. M., Enderby, J. E. and Egelstaff, P. A., *J. Phys. C.* **1**, 784 (1968).
9. Vineyard, G. H., *Phys. Rev.* **96**, 93 (1954).
10. Blech, I. A. and Averbach, B. L., *Phys. Rev.* **137**, A1113 (1965).
11. Bacon, G. E., " Neutron Diffraction ", Clarendon Press, Oxford, 1962.
12. Guinier, A., " X-ray Diffraction ", W. H. Freeman and Co., San Francisco and London, 1963.
13. Norman, N., *Acta Cryst.* **10**, 370 (1957).
14. Krogh-Moe, J., *Acta Cryst.* **9**, 951 (1956).
15. Hansen, M., " Constitution of Binary Alloys ", McGraw-Hill Book Co. Inc. N.Y., 1958.
16. Oehme, H. and Hauschild, J., *Kerntechnik* **8**, 205 (1966).
17. Bühner, H F. and Steeb, S., *Z. Metallkde.* **62**, 27 (1971).
18. Dutchak, Ya. I., *Fiz. metal. metalloved.* **9**, 314 (1960).
19. Müller, H. K. F. and Hendus, H., *Z. Naturf.* **12a**, 102 (1957).
20. Lashko, A. S. and Poltavtsev, Y. G., *Soviet Phys. Cryst.* **13**, 287 (1968).
21. Waseda, Y. and Suzuki, K., *Phys. Letters* **35A**, 315 (1971).
22. Wagner, C. N. J., Ocken, H. and Joshi, M. L., *Z. Naturf.* **20a**, 325 (1965).
23. Steeb, S. and Hezel, R., *Z. Physik* **191**, 398 (1966).
24. Steeb, S. and Bühner, H. F., *Z. Naturf.* **25a**, 1737 (1970).
25. Bienias, A. and Sauerwald, F., *Z. anorg. allg. Chem.* **161**, 51 (1927).
26. Dutchak, Ya. I. and Panasyuk, P. V., *Fiz. metal. metalloved.* **18**, 155 (1964).

Downloaded At: 09:02 28 January 2011